Brain Structure and Function
https://doi.org/10.1007/s00429-021-02305-9

ORIGINAL ARTICLE

Intra- and interhemispheric symmetry of subcortical brain structures: a volumetric analysis in the aging human brain

Jaime Gómez-Ramírez[1] · **Javier J. González-Rosa**[2,3]

Received: 22 February 2021 / Accepted: 19 May 2021

Abstract
Here, we address the hemispheric interdependency of subcortical structures in the aging human brain. In particular, we investigated whether subcortical volume variations can be explained by the adjacency of structures in the same hemisphere or are due to the interhemispheric development of mirror subcortical structures in the brain. Seven subcortical structures in each hemisphere were automatically segmented in a large sample of 3312 magnetic resonance imaging (MRI) studies of elderly individuals in their 70s and 80s. We performed Eigenvalue analysis, and found that anatomic volumes in the limbic system and basal ganglia show similar statistical dependency whether considered in the same hemisphere (intrahemispherically) or different hemispheres (interhemispherically). Our results indicate that anatomic bilaterality of subcortical volumes is preserved in the aging human brain, supporting the hypothesis that coupling between non-adjacent subcortical structures might act as a mechanism to compensate for the deleterious effects of aging.

Keywords MRI · Hemispheric asymmetry · Laterality · Aging · Eigenvalues · PCA

Introduction

The interest and use of understanding the differences between the two brain hemispheres go back a long way (Lashley 1958; Sperry 1984; LeDoux et al. 2020). Two of the most revelatory discoveries are the Broca area and Sperry split-brain experiments. Broca found that a patient who could only utter the syllable "tan" had a large lesion in the left posterior inferior frontal gyrus that was subsequently named the Broca's area (Ocklenburg and Gunturkun 2012). Hemispheric asymmetry and its importance in cognition acquired a dramatic turn with Sperry's split-brain experiments in cats, monkeys, and later on epileptic patients. Sperry showed that disconnecting the two hemispheres by severing the corpus callosum resulted in making the two hemispheres functionally independent (Sperry 1961).

✉ Jaime Gómez-Ramírez
jd.gomezramirez@gmail.com

[1] Instituto de Salud Carlos III, Madrid, Spain

[2] Department of Psychology, Universidad de Cádiz, Cádiz, Spain

[3] Instituto de Investigación Biomédica de Cádiz (INIBICA), Cádiz, Spain

However, and as it could not be otherwise given the staggering complexity of the brain, the lateralizations, and anatomic asymmetries cannot be accounted for within a simple narrative, for example, the left–right dominance (Nielsen et al. 2013) and conclusions may vary depending on the methodology applied, and the brain region or systems of interest. For instance, the increasing availability of data from volumetric brain imaging has made it possible to study the effect of lateralized functions on subcortical asymmetries (Morillon et al. 2010; Kang et al. 2015; Rane et al. 2017; Narvacan et al. 2017; Núñez et al. 2018; Esteves et al. 2019) and to postulate lateralization alterations as potential endophenotypic markers in chronic brain disorders such as schizophrenia (Dennison et al. 2013; Roalf et al. 2015; Okada et al. 2018) and other brain conditions, including Alzheimer's disease (Giannakopoulos et al. 1994), dyslexia (Leonard and Eckert 2008) and autism (Floris et al. 2020).

Evolutionary biology explains lateralization in the brain as a trade-off between bilateral symmetry and hemispheric asymmetry to cope with the external world. As suggested by Palmer (2004), bilateral symmetry may be the default condition, noticing that the mid-plane of developing organisms has anterior–posterior and dorso-ventral axes but there is no left–right axis. In a world in which predators may come from either side—right and left—sensory asymmetry could

Published online: 05 June 2021

come with the high price of being more vulnerable to predators approaching from the weak side. Along these lines, bilateral symmetry could be the result of natural adaptation. Nevertheless, the brain and other organs count with left-right asymmetries, such asymmetries could have evolved when proving to be more adaptive to the environment. For example, bilateral symmetry in limbs and legs is adaptive because it can produce linear movement. Thus, directional locomotion impinges a front–back asymmetry conserving the left–right symmetry.

Sensorimotor processing in the brain is overall organized symmetrically; however, asymmetries such as handedness are compatible with the cerebral organization (Corballis 2009; Willems et al. 2010; Neubauer et al. 2020). Whether intrahemispheric coupling is more predominant than bilateral symmetry, or lateralized interhemispheric components are more tightly coupled than intrahemispheric components, is still poorly understood (van der Knaap and van der Ham 2011).

Automatic segmentation of subcortical structures can produce important insights regarding the anatomic symmetric organization of the brain (Hervé et al. 2013; Kong et al. 2020). Subcortical structures are groups of neural formations deep within the brain, among these structures we find the limbic structures and the basal ganglia. The basal ganglia subcortical nuclei—caudate, putamen, pallidum—are located near the thalamus which is part of the limbic system. The limbic system refers to a group of subcortical nuclei—hypothalamus, thalamus, amygdala, hippocampus, accumbens—that supports a large variety of functions and behaviors such as long-term memory and affective responses (Shaw and Alvord Jr 1997; McLachlan 2009). The subcortical nuclei that compose the basal ganglia support motor control but they are also involved in motor learning, executive actions, and affective responses (Albin et al. 1989; Kreitzer and Malenka 2008). Age-related changes of the limbic system in normal populations have been shown using different imaging techniques, Diffusion Tensor Imaging (Gunbey et al. 2014), MRI (Callen et al. 2001; Fjell et al. 2015). However, a systematic and quantitative assessment, based on a large sample, of global symmetry in subcortical brain structures in the elderly brain is still missing.

In this study, we perform volumetric segmentation in over 3000 magnetic resonance imaging (MRI) studies in healthy elderly subjects, obtaining the volumetric estimation of the following seven subcortical structures: caudate, pallidum, putamen, thalamus, hippocampus, amygdala, and accumbens. Both global and lateralized subcortical brain symmetry are quantitatively assessed using correlation matrices and Eigenvalue analysis.

The rationale of selecting subcortical structures across and within hemispheres is to determine whether correlation based on locus (vicinity of structures) or genus (type of structure) is maintained in the brain of elderly subjects. In particular, we investigate whether volumetric variation can be explained with adjacency of structures in the same hemisphere, or is due to interhemispheric development of mirror subcortical structures in the brain.

Methodology

The dataset used here comes from a single-center, observational cohort study (Gómez-Ramírez et al. 2020a). The participants are home-dwelling elderly volunteers, aged in their 70s and 80s, without relevant psychiatric, neurological, or systemic disorders. Of the initial 1213 subjects, those who were diagnosed with MCI or dementia plus those lacking a brain MRI were excluded from our analysis, resulting in a cohort of 890 healthy elderly subjects. The subjects were assessed yearly for a total of five years resulting in 3312 assessments, with the number of yearly visits per subject varying from 2 to 5.

After signing informed consent, the participants undertake a yearly systematic clinical assessment, including medical history, neurological, neuropsychological exam, blood collection, and brain MRI. Apolipoprotein E (APOE) genotype was studied with total DNA isolated from peripheral blood following standard procedures. Ethical approval was granted by the Research Ethics Committee of *Instituto de Salud Carlos III*, and written informed consent was obtained from all the participants. The authors assert that all procedures contributing to this work comply with the ethical standards of the relevant national and institutional committees on human experimentation, and with the Helsinki Declaration of 1975 and its later amendments.

Imaging study

The imaging data were acquired in the sagittal plane on a 3T General Electric scanner (GE Milwaukee, WI) utilizing T1-weighted inversion recovery, supine position, flip angle 12∘, 3D pulse sequence: echo time *Min. full*, time inversion 600 ms., Receiver Bandwidth 19.23 kHz, field of view = 24.0 cm, slice thickness 1 mm and Freq × Phase 288 × 288. The preprocessing of MRI 3 Tesla images in this study consisted of generating an isotropic brain image with non-brain tissue removed. We used the FreeSurfer pipeline (recon-all FreeSurfer cortical reconstruction and parcellation process 2017) as the initial preprocessing step in the computational segmentation procedure. The postprocessing was performed with FreeSurfer (Fischl 2012), version freesurfer-darwin-OSX-ElCapitan-dev-20190328-6241d26 running under Mac OS X, product version 10.14.5.

FreeSurfer includes tools for processing structural MRI, functional MRI, diffusion MRI and PET data. Here, we

are focusing on structural MRI, in particular subcortical segmentation. The cross-sectional analysis starts with the surface-based stream (Dale et al. 1999; Fischl et al. 1999), where the skull is stripped, the cerebellum and brain stern are removed, the two hemispheres are separated and brain voxels are classified as white matter or gray matter and CSF (Fischl et al. 2002, 2004). Then, the volume-based stream segments the different subcortical structures of the brain using a subject-independent probabilistic atlas. The FreeSurfer training set consists of 40 MRIs, spread in age (10 healthy young subjects, 10 healthy middle-aged subjects, and 10 healthy elderly subjects) and including pathological brains (10 subjects with AD) (Desikan et al. 2006).

The stages in the FreeSurfer pipeline (in order) are surface-based stream, with skull-stripping cerebellum and brain stern removal, two hemispheres separation, and brain voxels classification (white matter, gray matter, and CSF), and finally brain segmentation, cortical and subcortical. The subcortical segmentation includes seven structures in each hemisphere, namely, thalamus, putamen, hippocampus, caudate, pallidum, amygdala, and accumbens.

For the sake of illustration, Fig. 1 shows the intracranial volume segmentation obtained for four subjects in the study out of a total of 3312 MRI scans.

Anomaly detection with the Isolation Forest algorithm

One premise of big data applied to brain imaging research is that given enough data, we may be able to characterize brain atrophy and fit the data to a model that makes predictions about the dynamics of the atrophy, that is, not only identify atrophy but also its progression in an individual basis.

Manual segmentation of the brain is a time-consuming and prone to error task (Vos et al. 2019; Despotović et al. 2015; Firbank et al. 2008; Collier et al. 2003). The segmentation of one volume may require an entire day of work from a dedicated expert. Hence, the use of manual segmentation on a dataset as ours, in the order of thousands of MRI scans, is not an option. The main advantages of automatic procedures are at least two: i) the lack of bias inherent in manual segmentation, two different human experts may produce very different estimates for the same image, and ii) automatic procedures are time-saving. On the other hand, automated quality control is paramount to avoid the inclusion of inaccurate measurements in the posterior analysis. Anomaly detection (Chandola et al. 2009) is an established approach in data analysis to identify observations with suspicious statistical properties when compared to the majority of data.

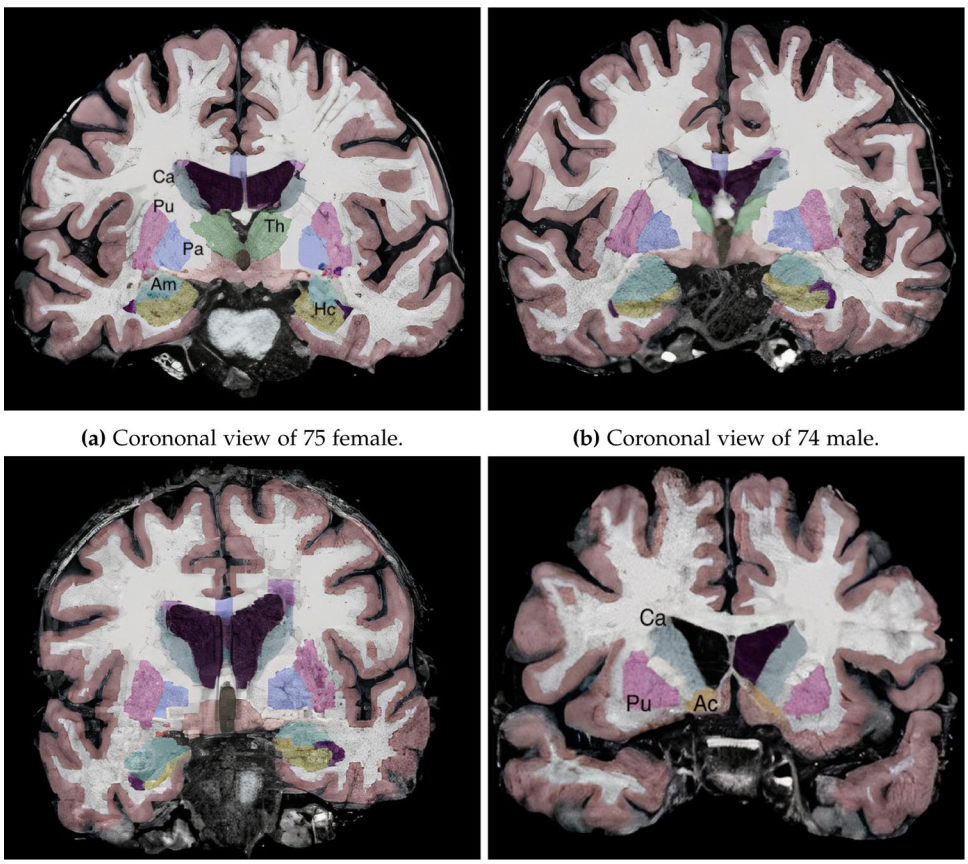

(a) Corononal view of 75 female. **(b)** Corononal view of 74 male.

(c) Corononal view of 76 female. **(d)** Corononal view of 80 female.

Fig. 1 Coronal view of the subcortical segmentation realized in 4 different subjects in the study. **a**, **d** contain the labels of the subcortical structures-clusters of cell bodies buried in white matter area; Ca: Caudate, Pu: Putamen, Pa: Pallidum, Th: Thalamus, Am: Amygdala, Hp: Hippocampus and Ac: Nucleus Accumbens

Isolation Forest (Liu et al. 2008) is an ensemble method (Breiman 1996) that has shown strong performance as an outlier detector in a variety of datasets (Domingues et al. 2018; Alaverdyan 2019). The algorithm works by selecting features and randomly selecting a split value between the maximum and minimum values of the selected features. The number of splitting required to isolate a sample is equal to the path length from the tree's root node to the tree's leaf node. By averaging the path length over a forest of random forests, we get a measure of normality, specifically a forest with shorter path lengths for particular samples indicates that the samples are likely to be anomalies.

We perform anomaly detection using the scikit-learn Isolation Forest implementation (Pedregosa et al. 2011). The parameters number of estimators, number of samples, and contamination level are set to the default values.

Statistical analysis

Table 1 shows the description of the variables included in the study: age, sex, Apolipoprotein E (APOE), handedness, and the volumetric estimates of the subcortical structures for a total of 3312 MRI studies.

To investigate whether the conditions—sex, handedness, and Apolipoprotein E (APOE)—can explain the variance in the volumetric estimate of the difference between the left hemisphere (LH) and the right hemisphere (RH), we build a regression model for each subcortical structure and condition as shown in Eq. (1). Thus, we split the total variation of the dependent variable, the difference between the left and right hemisphere volume of each subcortical structure, into sources of variation to find out whether the independent variable (sex, Apolipoprotein E (APOE), handedness) has a significant effect on the dependent variable (interhemispheric volumetric difference of subcortical structures).

The OLS regression model is shown in Eq. (1)

$$S_{\mathrm{D}} = S_{\mathrm{L}} - S_{\mathrm{R}} \sim C(X) + C(H) + C(A), \tag{1a}$$

where S_{L} is the volume of the LH subcortical structure S, S_{R} is the volume of the RH subcortical structure S and S_{D} is the volumetric normalized difference between the two hemispheres in structure S. X, H and A represent the variables sex, handedness and Apolipoprotein E (APOE) respectively codified as categorical.

Aggregate correlation analysis

The correlation matrix describes the degree to which any pair of two random variables in a set of random variables tends to deviate from their expected values. Thus, the element i, j in the correlation matrix M, $M_{i,j}$ contains the correlation coefficient between the ith random variable

Table 1 The table shows the description of the variables included in the study

$N = 3312$	$\mu + \sigma$			Groups					
Age	76.51 + 0.64								
Sex	F, M 2128, 1184								
APOE	$\epsilon(23)\epsilon(23)$, $\epsilon(23)\epsilon 4$, $\epsilon 4\epsilon 4$ 2790, 502, 20								
Handedness	R, L, A 3139, 89, 84								
Vol (mm^3)	lTh	lPu	lAm	lPa	lCa	lHc	lAc		
Mean	5946.3	3917.0	1252.6	1700.8	3202.9	3527.2	457.1		
SD	615.6	470.2	187.5	235.6	438.4	373.1	87.7		
Vol (mm^3)	rTh	rPu	rAm	rPa	rCa	rHc	rAc		
Mean	5798.5	3952.2	1399.3	1632.8	3379.0	3608.5	459.1		
Std	554.3	468.6	204.7	228.9	470.3	400.4	85.4		

On top, the age—mean and standard deviation—followed by the sex of the participants—64% of women—the Apolipoproteine4 frequency—$\epsilon 2$, $3\epsilon 2$, 3 (84.2%), $\epsilon 3\epsilon 4$ (15.2%), $\epsilon 4\epsilon 4$ (0.6%)—and the handedness—right handed (95%), left handed (2.6%) and ambidextrous (2.4%)

and the *j*th one. The correlation matrix can be computed from the covariance matrix if we are interested in both the strength and direction of the linear relationship between any pair of variables in the dataset. The correlation matrix is, thus, a collection of correlation coefficients expressing the standardized covariance between variables in a dataset.

To study whether statistical dependence between structures can be explained based on contiguity of structures (intrahemispheric) or in terms of the bilateral development of the brain (interhemispheric), we extract from the correlation matrix ρ that contains the correlation coefficients between all variables, three correlation matrices, two intrahemispheric and one interhemispheric. Accordingly, from ρ, we obtain ρ_R or the correlation matrix of the structures located in the right hemisphere, ρ_L or the correlation matrix of the structures in the left hemisphere, and the bilateral correlation matrix ρ_B which contains the correlation between any pair of structures as long as they are in different hemispheres. All three matrices ρ_L,ρ_R, and ρ_B are $7x7$ dimensional and the correlation matrix ρ is 14×14 dimensional. This is shown schematically in Table 2.

A first approximation to assess the overall strength of a correlation matrix could be done by averaging all the correlation coefficients, however, the average correlation will be biased and the average will tend to underestimate the true correlation. The Fisher transformation can overcome this problem and yield an unbiased estimate by performing the Z transformation of the correlation matrix, and then inverse transform the average. Formally, given the correlation coefficient r between two variables, the Fisher's z-transformation of r and the inverse transformation is as follows: Fisher z-transformation:

$$z = \frac{1}{2} ln(\frac{1+r}{1-r}) = arctan(r), \tag{2a}$$

$$r = \frac{e^{2z}-1}{e^{2z}+1} = tanh(z). \tag{2b}$$

Accordingly, the total correlation of the intrahemispheric correlation matrices (ρ_L, ρ_R) and the interhemispheric correlation matrix (ρ_B) shown in Table 2 can be estimated using the Fisher z-transformation as shown schematically in Eqs. 3a, 3b and 3c.

$$P_{\mathrm{L}} = \tan h(\arctan h(\bar{\rho_L})), \tag{3a}$$

$$P_{\mathrm{R}} = \tan h(\arctan h(\bar{\rho_R})), \tag{3b}$$

$$P_{\mathrm{B}} = \tan h(\arctan h(\bar{\rho_B})). \tag{3c}$$

Table 2 Decomposition of the correlation matrix into three submatrices, ρ_L selects pair of structures in the left hemisphere, ρ_R is the selection of pair of structures in the right hemisphere, and ρ_B is the correlation matrix of pair of structures located in different hemispheres

ρ	LH	RH
LH	ρ_L	ρ_B
RH	ρ_B	ρ_R

Eigenvalue analysis

Since eigenvectors and eigenvalues uniquely define the covariance matrix, we can represent the covariance matrices in Table 2 by its eigenvectors and eigenvalues and therefore gain an understanding of the shape of the dataset.

We can map the $n(n-1)/2$ correlations among n variables in a correlation matrix into n eigenvalues and their associated eigenvectors, with the eigenvalues being linear functions of the underlying correlations. Importantly, when all correlations are positive, the first eigenvalue is approximately a linear function of the average correlation among the variables and tells us the amount of variance in the correlation matrix that can be accounted for with a linear model by a single underlying factor. We can naturally extend this idea to the second, third, and so on, eigenvalues. Once we have computed the eigenvalues λ_i of a correlation matrix, we can compute the area defined by the cumulative eigenvalue function as an aggregate measurement of the total cumulative percentage of variance retained by each dimension (Eq. 4).

$$S = \int_{\lambda_1}^{\lambda_n} F(\lambda) \mathrm{d}\lambda. \tag{4a}$$

We can calculate the S_L, S_R and S_B for each correlation matrix shown in Table 2, the cumulative curve $F(\lambda)$ would indicate the independence of the variables within each matrix, that is, the degree of independence of the subcortical structures in each hemisphere (S_L, S_R) and interhemispherically (S_B).

Results

We use the Isolation Forest Algorithm (Liu et al. 2008) to remove outliers in the dataset using the sklearn implementation (Pedregosa et al. 2011). Isolation Forest is an unsupervised learning algorithm for detecting anomalies. The algorithm explicitly isolates anomalous points in the dataset rather than detecting points that fall outside the "normal" profile. From the dataset free of anomalies detected by the algorithm, we select the cases diagnosed as healthy, that is to say, cases with a diagnosis of mild cognitive impairment

or Alzheimer's disease are removed to deal only with elderly healthy brains (See Supplemental Methods). The resulting dataset makes a total of 3312 MRI scans of healthy brains segmented to estimate the volume of seven subcortical structures, namely Thalamus, Putamen, Amygdala, Pallidum, Caudate, Hippocampus and Nucleus Accumbens.

Figure 2 shows the volume estimates of the subcortical structures. The structure with the largest volume is the Thalamus, followed by Putamen, Hippocampus, Caudate, Pallidum, Amygdala and lastly Accumbens. The size of the same structure in either hemisphere is very similar. For example, the mean distribution of the percentage difference between the right and the left hemisphere is −1.47% Thalamus, 0.3% Putamen, 0.8% Hippocampus, 1.76% Caudate, 1.38% Pallidum, 1.57% Amygdala and 0.02% Nucleus Accumbens. The right hemisphere volume is on average slightly larger than the left hemisphere volume for all structures except the Thalamus.

In the analysis presented in Table 3, we focus on the effect of sex, Apolipoprotein E (APOE), and handedness in the preservation of symmetry for each subcortical structure, calculated as the difference between the volume for each hemisphere of the same structure (Eq. 1). We fit a regression model for each bilateral structure (thalamus, putamen, amygdala, pallidum, caudate, hippocampus, caudate) and conditions (sex, Apolipoprotein E (APOE), and handedness). For the sake of simplicity, we show only the Prob (F-statistic) from the OLS regression results. Since the data are not balanced (different sample sizes for each group), we perform a type 3 sums of squares analysis. Both type 2 and type 3 sums of squares yield similar results (Seabold and Perktold 2010) which is due to the fact that the underlying

Table 3 Table with the analysis of variance using the F test to determine whether the variability between group means is larger than the variability of the observations within the groups

$P(F$-statistic)	Sex	APOE	Handedness
Thalamus_D	***		***
Putamen_D	***		*
Amygdala_D	***		
Pallidum_D	***		**
Caudate_D	***		*
$\text{Hippocampus}_\text{D}$	***		***
$\text{Accumbens}_\text{D}$			

All the structures except the accumbens show significant bilateral volumetric difference between the two sexes ($P << 0.001$). No structure is found to have significant differences ($P < 0.01$) among the three forms of Apolipoprotein E (APOE)—no $\epsilon 4$ allele inherited, one $\epsilon 4$ allele, and 2 $\epsilon 4$ alleles inherited from both parents. Regarding handedness, thalamus and hippocampus ($P < 0.001$) show significant differences between the three groups—right handed, left handed and ambidextrous

*$P < 0.05$

**$P < 0.01$

***$P < 0.001$

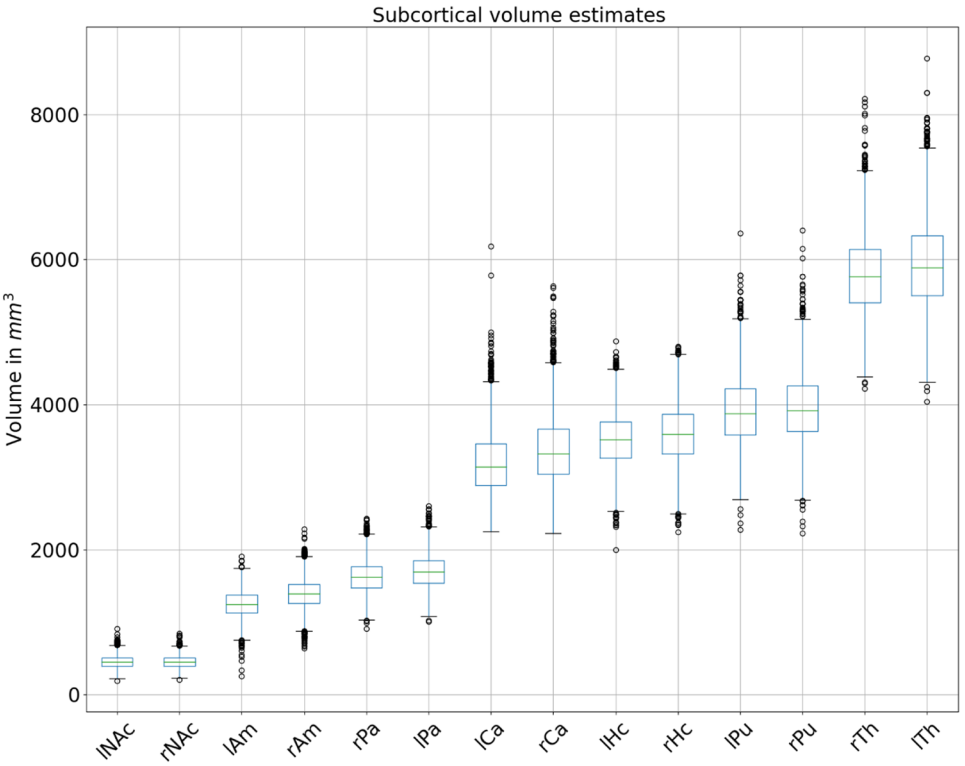

Fig. 2 Boxplot of the seven bilateral subcortical structures segmented with FreeSurfer for 3312 healthy subjects. The estimated median volumes from the smallest to the largest structure are as follows: Accumbens R/L 459.10/457.10 mm^3, Amygdala R/L 1399.31/1252.65 mm^3, Pallidum R/L 1632.85/1700.82 mm^3, Caudate R/L 3379.04/3202.93 mm^3, Hippocampus R/L 3312.00/3312.00 mm^3, Putamen R/L 3952.21/3916.95 mm^3, Thalamus R/L 5798.49/5946.30 mm^3

assumption of type 2 of no interactions between factors holds (Langsrud 2003).

The results support the hypothesis of sex-related differences in the symmetry of subcortical structures studied with the only exception of accumbens and amygdala. Studies of sex differences in the relative volume of subcortical structures have produced conflicting results with studies reporting differences in putamen, hippocampus, amygdala, thalamus, and pallidum (Ruigrok et al. 2014), while Ritchie et al. (2018) found no statistically significant differences in the hippocampus, caudate, and thalamus after adjusting for the difference in total brain size between men and women. The inconsistencies found in the literature on sex differences can be motivated by the use of different types of MRI scans, segmentation algorithms, statistical analysis, size and characteristics of the sample, etc (Herron et al. 2015). The present study is single center with an identical protocol for image acquisition, image segmentation, and postprocessing. Thus, our results are relatively impervious to lack of consistent findings due to differences in the magnetic field strength of the MRI scanner, or differences in the quantification methods of segmentation. Furthermore, the potential problems of age-related changes in subcortical volume are reduced by addressing a large sample of elderly subjects in their seventies and eighties.

The correlation matrix ρ of the 14 structures automatically segmented is shown in Fig. 3. The correlation coefficient of the same structure across the two hemispheres (adjacent cells of the main diagonal) is larger than between any two other structures. The two smallest structures, the amygdala, and the nucleus accumbens are also the two structures with the weaker correlation coefficient .68 and .66, respectively, while the rest of the structures are above 0.8. The accumbens happens to be also the structure that shows on average the least statistical dependence with the rest of the structures (the last two rows in Fig. 3). The hippocampus and the amygdala are the two structures with the strongest correlation; this holds true for the three correlation matrices; the maximum value, excluding the principal diagonal, is always for the amygdala, hippocampus pair. Regarding the correlation matrix of interhemispheric structures, the ranking of bilateral correlation in decreasing order is as follows: Caudate, Putamen, Thalamus, Hippocampus, Pallidum, Amygdala, and Accumbens. Always the strongest correlation is for the bilateral structures ($\rho(x_L, x_R) > \rho(x_L, y_R), \forall y \neq x$), that is, the statistical dependence between the same left and the right structure (x) is larger than for any two different structures (x, y).

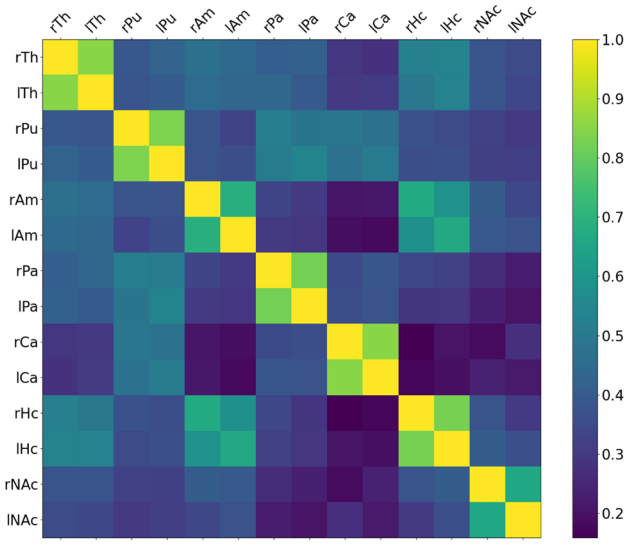

Fig. 3 Correlation matrix of the seven bilateral subcortical structures segmented with FreeSurfer. The elements of the diagonal are naturally 1, the correlation matrix seems to indicate that the strongest statistical dependence is for the inter hemispheric correlation of the same structure

Admittedly, the three 7×7 submatrices shown in Table 2 do not contain any additional information, that is, not already included in the 14×14 correlation matrix ρ shown in Fig. 3. The rationale of selecting structures across and within hemispheres is to acquire both intrahemispheric and interhemispheric views of the brain. By isolating the study of statistical dependence in a single hemisphere versus the entire span, we can establish whether the volume variation of the different subcortical structures is better explained locally (i.e., spatial proximity structure in the same hemisphere) or globally (i.e., connection across hemispheres).

We are, thus, interested in acquiring a systemic view of the statistical dependency among subcortical structures. To that end, we need to understand how their volumes are related according to their hemispheric location. As shown in Table 2, it is possible to extract the correlation matrices for each hemisphere and the bilateral case. However, a correlation matrix is a list of correlation coefficients, when what we need is an aggregate of the overall correlation for each matrix. As discussed in the Methodology section, we cannot compute the average of the correlation matrix because correlation coefficients are not additive. However, an approximation of the overall strength of a correlation matrix can be calculated by computing the Fisher's z-transformation of coefficient r in the correlation matrix, averaging the total to finally compute the inverse transformation (Eq. 3). The result of applying the Fisher's z-transformation to obtain the overall correlation in the bilateral, left hemisphere, and right hemisphere correlation matrices is shown in Fig. 4.

We finalize our investigation of the intrahemispheric versus interhemispheric statistical dependence of subcortical brain structures with principal component analysis (PCA) of the three correlation matrices ρ_L,ρ_B, and ρ_B (Table 2). The eigenvectors and eigenvalues of the data covariance matrix allow us to find the principal components in order

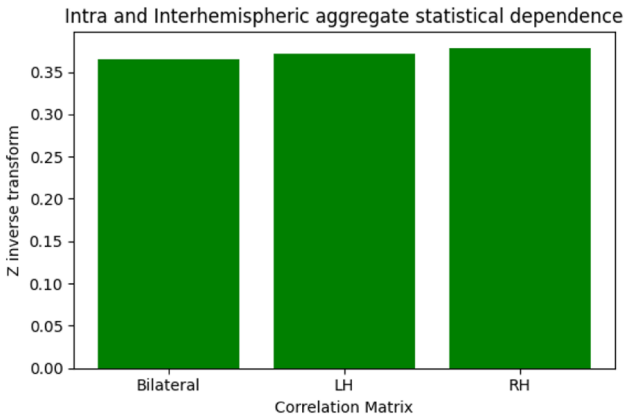

Fig. 4 Aggregate statistical dependence for interhemispheric and intrahemispheric subcortical volume estimates computed with the Z inverse transformation (Eq. 3). The statistical dependence is remarkably similar in all three cases. Of note, the main diagonal has been excluded from the computation of the Z transformation to avoid bias towards the interhemispheric matrices which are symmetric, while the bilateral correlation matrix is not symmetric

of significance. Thus, the first eigenvalue is the variance of the first principal component, the second of the second component and so on.

The distribution of the eigenvalues calculated for each correlation matrix are shown in Fig. 5. Next, to assess the degree of independence of the structures volume, intra- and interhemispheric, we compute the area defined under the curve defined by the cumulative eigenvectors shown in Fig. 5. The area under the curve described by the cumulative eigenvalues is computed using the trapezoidal integration rule, i.e., dividing the total area into many trapezoids that yield the approximated area.

The area defined for the eigenvalues in the bilateral matrix is slightly larger for the interhemispheric correlation matrix, $B = 0.7143, L = 0.6795 R = 0.6794$. Thus, the area of the left and right hemispheres renders almost identical results, while the cumulative eigenvalues relative area for the bilateral correlation matrix is only 5% larger. The amount of information both unilaterally and bilaterally is, therefore, similar. Note that if the data were independent,

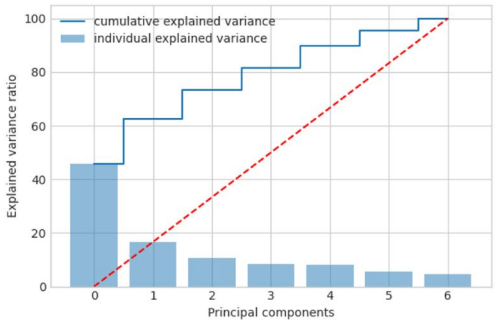

(a) Cumulative eigenvalue distribution for Left Hemisphere correlation matrix

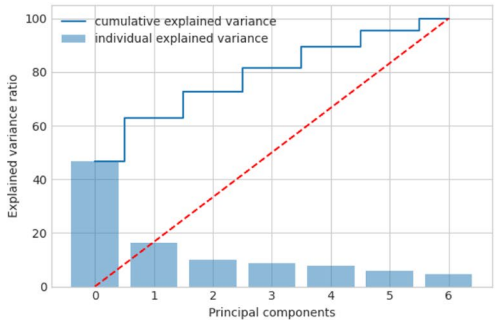

(b) Cumulative eigenvalue distribution for Right Hemisphere correlation matrix

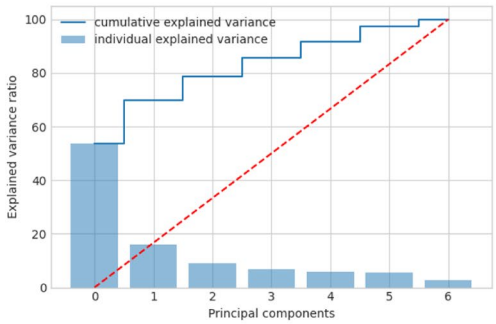

(c) Cumulative eigenvalue distribution for bilateral (Left vs Right structures) structures.

Fig. 5 The eigenvalues explain the variance of the data along the eigenvectors (principal components). The figure shows the explained variance of each of the correlation matrices by depicting the cumulative eigenvalue (y-axis) versus the order of eigenvalues (x-axis). The explained variance can be calculated from the eigenvalues and tells us how much information (variance) can be attributed to each of the principal components. From the figure, we can deduce that the subcortical structures have the same statistical dependence when studied intrahemispherically (**a**, **b**) and comparable with the interhemispherical eigenvalue analysis (**c**)

then the cumulative curve would have an area of .5 as shown in the discontinuous red line in Fig. 5. The important point to be retained is that the volumetric estimates of subcortical structures when taken either bilaterally or unilaterally show similar statistical dependence.

Discussion and conclusions

Imaging studies in the order of thousands of MRIs performed in the same center and using identical protocol and equipment are very costly. While it is possible to build aggregates of large datasets combining images from different imaging centers, issues related to the consistency of the results need to be carefully addressed.

We leverage a large single-center dataset of segmented subcortical structures to foster our understanding of the anatomic symmetric organization of the brain. Over 3000 MRI scans obtained in the same center and using identical procedure were segmented to extract the volume of seven subcortical structures in the limbic system and the basal ganglia, namely thalamus, putamen, hippocampus, caudate, pallidum, amygdala, and accumbens. While several studies that compare variations in volume and alterations of symmetry in relation to the sexes, handedness (Ocklenburg and Gunturkun 2012; Kang et al. 2015; Guadalupe et al. 2017), language (Corballis 2009), or even as potential markers in brain disorders such as schizophrenia (Roalf et al. 2015) exist, the study of the systemic volumetric interdependencies of subcortical structures has not received sufficient attention.

There are a large number of studies of sex differences in subcortical structures as well as studies that investigate the effect of Apolipoprotein E $\epsilon 4$ (Fleisher et al. 2005; Tang et al. 2015) handedness (Szabó et al. 2003) and other factors on the volume of brain structures (See Supplemental Results and references therein for an analysis of the effect of sex and age in subcortical volumetric estimates). We find no detectable effect on subcortical asymmetries when the sample is separated based on the allele $\epsilon 4$. Statistical tests found handedness-related asymmetries in the thalamus and hippocampus with no effect in accumbens and putamen. A recent meta-analysis (Guadalupe et al. 2017) did not find a significant effect of handedness on subcortical asymmetries; however, the same study found that asymmetry of certain structures, e.g., the putamen, varies with age. Finally, sex has a strong effect on the subcortical volumetric asymmetry in all structures except for the accumbens. This is in agreement with Bayesian hypothesis testing performed on 5216 participants in the UK Biobank (Ritchie et al. 2018) where no difference was found for the bilateral nucleus accumbens, finding, on the other hand, evidence for the hypothesis of difference for all other regions.

Sex differences in brain structures are thought to reflect biological and environmental influences which impinge upon brain development throughout the lifespan. Dimorphism or the condition by which the two sexes exhibit different characteristics beyond the differences in their sexual organs has been reported in the human brain. Sexual dimorphism has been found in brain tissue composition (Allen et al. 2003), cortical thickness, (Goldstein et al. 2001; Chiarello et al. 2009), and in subcortical structures morphometry (Lotze et al. 2019). Additionally, sex-related differences are found in brain activation and connectivity patterns (Ingalhalikar et al. 2014). A recent cross-sectional MRI study examining brain maturation (Duerden et al. 2020), found sex-based differences in cortical thickness and surface area measures, particularly in frontoparietal regions, whilst subcortical structures presented only minor differences between males and females. These findings overall seem to suggest that subcortical surface area expansion could be associated with age-related maturation changes and linked to dendritic and synaptic architecture alterations underlying the brain changes during different stages of life.

A better understanding of sexual diphormism in the brain will require a whole-brain framework that can accommodate factors such as sex-based genetic expression (Kang et al. 2011), sex differences in the endocrine system, in particular, steroid hormones (Giedd et al. 2012) together with appropriate models that incorporate, for example, factors related with child care and maternal health. The influence of sex on brain asymmetry and lateralization has been studied from the temporal perspective provided by developmental and maturational processes in the brain. While neuroanatomic data have shown sex-related differences in infancy and childhood (Caviness Jr et al. 1996; Knickmeyer et al. 2008) which remain relatively stable during the adult years (Goldstein et al. 2001), we lack a clear understanding of sexual dimorphism in the aging brain (Király et al. 2016). An intriguing hypothesis is the reversal of cerebral sexual dimorphism in mental disorders such as schizophrenic psychosis (Mendrek 2007). For example, in Egloff et al. (2018), researchers found reversed sexual dimorphism only in the hippocampus, with the rest of subcortical volumes unaffected.

The symmetric pattern of subcortical volumetric changes found in this study could suggest age and sex interactions at play in the rebalancing of developmental and sex-related differences in subcortical areas across the lifespan. The present study is, thus, interested in the characterization of the interdependency of subcortical structures in healthy, elderly brains. We propose a methodology based on Eigenvalue analysis to estimate the aggregate correlation of volumetric subcortical structures when they are studied in either the same hemisphere and in different hemispheres. While there is abundant literature in cortical and subcortical structural variation associated with

biological (Eyler et al. 2011; Nickl-Jockschat et al. 2012; Wen et al. 2016; Bas-Hoogendam et al. 2018) and socioeconomic factors (Jenkins et al. 2020), the effect of aging on both the intrahemispheric and the interhemispheric symmetry of subcortical structures is inadequately understood.

To our knowledge, this is the largest single-center study of subcortical global symmetry. We find that the seven structures studied have similar coupling when their volumes are studied either interhemispherically or intrahemispherically. The correlation matrix of all the structures segmented show that the statistical dependence for any given structure is always the largest with its twin structure in the other hemisphere. Along these lines, we could say that development is more important than hemispheric proximity.

Interhemispheric integration is inevitable for how the brain develops and grows (Gazzaniga 2000). Both hemispheric specialization and hemispheric integration are to be expected and are found in our results. By decomposing the correlation matrix into three submatrices containing the pairwise correlations both within the same hemisphere and in different hemispheres, we set apart three different views—left hemisphere, right hemisphere, and interhemispheric—of the statistical dependency between subcortical structures in the brain.

The aggregate statistical dependence for interhemispheric and intrahemispheric subcortical volume estimates are computed using two methods. First, directly from the correlation matrix via the Z inverse transformation (Eq. 3) and last, using Eigenvalue analysis to compute the cumulative curve of the distribution of the eigenvalues that would indicate the independence of the variables within each matrix. In either case, the statistical dependence is remarkably similar, indicating that the subcortical structures studied here have comparable coupling when taken as a whole for each hemisphere and when taken in different hemispheres.

The study overall indicates that anatomic bilateral symmetry is preserved in the aging human brain, supporting recent findings that postulate increased communication between distant brain areas as a mechanism to compensate for the deleterious effects of aging (Davis et al. 2017). The characterization of brain subcortical symmetry proposed here allows new views of interhemispheric and intrahemispheric volume variation, setting the basis for future studies of anatomical symmetry and asymmetry in healthy brain aging.

Supplementary Information The online version contains supplementary material available at https://doi.org/10.1007/s00429-021-02305-9.

Acknowledgements The authors would like to thank the generous persons that volunteered to participate in the study and *Fundación Reina Sofía* for their support. The authors acknowledge funding from *Ministerio de Ciencia, Innovación y Universidades* (CONNECT-AD) RTI2018-098762-B-C31 and Structural Funds ERDF (INTERREG V-A Spain-Portugal (POCTEP) Grant: 0348CIE6E).

Author Contributions JG-R conceived the idea, collected data, and wrote the manuscript. JG-R with inputs from JJG-R designed the modeling and performed the statistical analysis. JJG-R analyzed and interpreted the results, wrote and supervised the manuscript.

Declarations

Data and code availability The data set can be downloaded from https://github.com/grjd/bilateralbrain .

Conflict of interest The authors declare no competing interests.

References

Alaverdyan Z (2019) Unsupervised representation learning for anomaly detection on neuroimaging. Application to epilepsy lesion detection on brain MRI. PhD thesis, Université de Lyon

Albert MS, DeKosky ST, Dickson D, Dubois B, Feldman HH, Fox NC, Gamst A, Holtzman DM, Jagust WJ, Petersen RC et al (2011) The diagnosis of mild cognitive impairment due to Alzheimer's disease: recommendations from the national institute on aging-Alzheimer's association workgroups on diagnostic guidelines for Alzheimer's disease. J Alzheimer's Assoc 7(3):270–279

Albin RL, Young AB, Penney JB (1989) The functional anatomy of basal ganglia disorders. Trends Neurosci 12(10):366–375

Allen JS, Damasio H, Grabowski TJ, Bruss J, Zhang W (2003) Sexual dimorphism and asymmetries in the gray-white composition of the human cerebrum. Neuroimage 18(4), 880–894

Bas-Hoogendam JM, van Steenbergen H, Tissier RL, Houwing-Duistermaat JJ, Westenberg PM, van der Wee NJ (2018) Subcortical brain volumes, cortical thickness and cortical surface area in families genetically enriched for social anxiety disorder-a multiplex multigenerational neuroimaging study. EBioMedicine 36:410–428

Bauer E, Toepper M, Gebhardt H, Gallhofer B, Sammer G (2015) The significance of caudate volume for age-related associative memory decline. Brain Res 1622:137–148

Breiman L (1996) Bagging predictors. Mach Learn 24(2):123–140

Callen D, Black SE, Gao F, Caldwell C, Szalai J (2001) Beyond the hippocampus: Mri volumetry confirms widespread limbic atrophy in ad. Neurology 57(9), 1669–1674

Caviness V Jr, Kennedy D, Richelme C, Rademacher J, Filipek P (1996) The human brain age 7–11 years: a volumetric analysis based on magnetic resonance images. Cereb Cortex 6(5):726–736

Chandola V, Banerjee A, Kumar V (2009) Anomaly detection: a survey. ACM Comput Surv (CSUR) 41(3):1–58

Chiarello C, Welcome SE, Halderman LK, Towler S, Julagay J, Otto R, Leonard CM (2009) A large-scale investigation of lateralization in cortical anatomy and word reading: are there sex differences? Neuropsychology 23(2):210

Collier DC, Burnett SS, Amin M, Bilton S, Brooks C, Ryan A, Roniger D, Tran D, Starkschall G (2003) Assessment of consistency in contouring of normal-tissue anatomic structures. J Appl Clin Med Phys 4(1):17–24

Corballis MC (2009) The evolution and genetics of cerebral asymmetry. Philos Trans R Soc B Biol Sci 364(1519):867–879

Dale A, Fischl B, Sereno MI (1999) Cortical surface-based analysis: I. Segmentation and surface reconstruction. NeuroImage 9(2):179–194

Davis SW, Luber B, Murphy DL, Lisanby SH, Cabeza R (2017) Frequency-specific neuromodulation of local and distant connectivity in aging and episodic memory function. Human Brain Map 38(12):5987–6004

Dennison M, Whittle S, Yücel M, Vijayakumar N, Kline A, Simmons J, Allen NB (2013) Mapping subcortical brain maturation during adolescence: evidence of hemisphere-and sex-specific longitudinal changes. Dev Sci 16(5):772–791

Desikan RS, Ségonne F, Fischl B, Quinn BT, Dickerson BC, Blacker D, Buckner RL, Dale AM, Maguire RP, Hyman BT et al. (2006) An automated labeling system for subdividing the human cerebral cortex on mri scans into gyral based regions of interest. Neuroimage 31(3): 968–980

Despotović I, Goossens B, Philips W (2015) Mri segmentation of the human brain: challenges, methods, and applications. Comput Math Methods Med 2015:450341

Domingues R, Filippone M, Michiardi P, Zouaoui J (2018) A comparative evaluation of outlier detection algorithms: experiments and analyses. Pattern Recogn 74:406–421

Duerden EG, Chakravarty MM, Lerch JP, Taylor MJ (2020) Sex-based differences in cortical and subcortical development in 436 individuals aged 4–54 years. Cerebral Cortex 30(5), 2854–2866

Egloff L, Lenz C, Studerus E, Harrisberger F, Smieskova R, Schmidt A, Huber C, Simon A, Lang UE, Riecher-Rössler A et al. (2018) Sexually dimorphic subcortical brain volumes in emerging psychosis. Schizophr Res 199:257–265

Esteves M, Moreira PS, Marques P, Castanho TC, Magalhães R, Amorim L, Portugal-Nunes C, Soares JM, Coelho A, Almeida A et al. (2019) Asymmetrical subcortical plasticity entails cognitive progression in older individuals. Aging Cell 18(1):e12857

Eyler LT, Prom-Wormley E, Fennema-Notestine C, Panizzon MS, Neale MC, Jernigan TL, Fischl B, Franz CE, Lyons MJ, Stevens A et al. (2011) Genetic patterns of correlation among subcortical volumes in humans: results from a magnetic resonance imaging twin study. Hum Brain Map 32(4):641–653

Firbank MJ, Barber R, Burton EJ, O'Brien JT (2008) Validation of a fully automated hippocampal segmentation method on patients with dementia. Hum Brain Map 29(12):1442–1449

Fischl B (2012) Freesurfer. Neuroimage 62(2):774–781

Fischl B, Salat DH, Busa E, Albert M, Dieterich M, Haselgrove C, van der Kouwe A, Killiany R, Kennedy D, Klaveness S, Montillo A, Makris N, Rosen B, Dale AM (2002) Whole brain segmentation: automated labeling of neuroanatomical structures in the human brain. Neuron 33:341–355

Fischl B, Sereno MI, Dale A (1999) Cortical surface-based analysis: II: inflation, flattening, and a surface-based coordinate system. NeuroImage 9(2):195–207

Fischl B, van der Kouwe A, Destrieux C, Halgren E, Sgonne F, Salat DH, Busa E, Seidman LJ, Goldstein J, Kennedy D, Caviness V, Makris N, Rosen B, Dale AM (2004) Automatically parcellating the human cerebral cortex. Cereb Cortex 14(1):11–22

Fjell AM, Sneve MH, Storsve AB, Grydeland H, Yendiki A, Walhovd KB (2015) Brain events underlying episodic memory changes in aging: a longitudinal investigation of structural and functional connectivity. Cereb Cortex 26:1272–1286

Fleisher A, Grundman M, Jack, Clifford R, J, Petersen RC, Taylor C, Kim HT, Schiller DHB, Bagwell V, Sencakova D, Weiner MF, DeCarli C, DeKosky ST, van Dyck CH, Thal LJ, Study ADC (2005) Sex, apolipoprotein E e4 status, and hippocampal volume in mild cognitive impairment. Arch Neurol 62(6):953–957

Floris DL, Wolfers T, Zabihi M, Holz NE, Zwiers MP, Charman T, Tillmann J, Ecker C, Dell'Acqua F, Banaschewski T et al (2020) Atypical brain asymmetry in autism—a candidate for clinically meaningful stratification. Biol Psychiatr Cogn Neurosci Neuroimaging (in press)

FreeSurfer cortical reconstruction and parcellation process (2017) Anatomical processing script: recon-all. https://surfer.nmr.mgh.harvard.edu/fswiki/recon-all. Accessed 30 May 2020

Gazzaniga MS (2000) Cerebral specialization and interhemispheric communication: does the corpus callosum enable the human condition? Brain 123(7):1293–1326

Giannakopoulos P, Bouras C, Hof PR (1994) Alzheimer's disease with asymmetric atrophy of the cerebral hemispheres: morphometric analysis of four cases. Acta Neuropathol 88(5):440–447

Giedd JN, Raznahan A, Mills KL, Lenroot RK (2012) magnetic resonance imaging of male/female differences in human adolescent brain anatomy. Biol Sex Differ 3(1):1–9

Goldstein JM, Seidman LJ, Horton NJ, Makris N, Kennedy DN, Caviness VS Jr, Faraone SV, Tsuang MT (2001) Normal sexual dimorphism of the adult human brain assessed by in vivo magnetic resonance imaging. Cereb Cortex 11(6):490–497

Gómez-Ramírez J, Ávila-Villanueva M, Fernández-Blázquez MÁ (2020a) Selecting the most important self-assessed features for predicting conversion to mild cognitive impairment with random forest and permutation-based methods. Sci Rep 10(1):1–15

Gómez-Ramírez J, Fernandez-Blazquez MA, González-Rosa J (2020b) A causal analysis of the effect of age and sex differences on brain atrophy in the elderly brain. bioRxiv. https://doi.org/10.1101/2020.11.20.391623

Guadalupe T, Mathias SR, Theo G, Whelan CD, Zwiers MP, Abe Y, Abramovic L, Agartz I, Andreassen OA, Arias-Vásquez A et al. (2017) Human subcortical brain asymmetries in 15,847 people worldwide reveal effects of age and sex. Brain imag Behav 11(5):1497–1514

Gunbey HP, Ercan K, Fındıkoglu AS, Bulut HT, Karaoglanoglu M, Arslan H (2014) The limbic degradation of aging brain: a quantitative analysis with diffusion tensor imaging. Sci World J 2014:196513

Herron TJ, Kang X, Woods DL (2015) Sex differences in cortical and subcortical human brain anatomy. F1000Research 4(88):88

Hervé P-Y, Zago L, Petit L, Mazoyer B, Tzourio-Mazoyer N (2013) Revisiting human hemispheric specialization with neuroimaging. Trends Cogn Sci 17(2):69–80

Hughes CP, Berg L, Danziger W, Coben LA, Martin RL (1982) A new clinical scale for the staging of dementia. Br J Psych 140(6):566–572

Ingalhalikar M, Smith A, Parker D, Satterthwaite TD, Elliott MA, Ruparel K, Hakonarson H, Gur RE, Gur RC, Verma R (2014) Sex differences in the structural connectome of the human brain. Proceedings of the National Academy of Sciences 111(2), 823–828

Jenkins LM, Chiang JJ, Vause K, Hoffer L, Alpert K, Parrish TB, Wang L, Miller GE (2020) Subcortical structural variations associated with low socioeconomic status in adolescents. Hum Brain Map 41(1), 162–171

Kang HJ, Kawasawa YI, Cheng F, Zhu Y, Xu X, Li M, Sousa AM, Pletikos M, Meyer KA, Sedmak G et al. (2011) Spatio-temporal transcriptome of the human brain. Nature 478(7370):483–489

Kang X, Herron TJ, Ettlinger M, Woods DL (2015) Hemispheric asymmetries in cortical and subcortical anatomy Laterality: asymmetries of Body, Brain Cogn 20(6):658–684

Király A, Szabó N, Tóth E, Csete G, Faragó P, Kocsis K, Must A, Vécsei L, Kincses ZT (2016) Male brain ages faster: the age and gender dependence of subcortical volumes. Brain Imag Behav 10(3):901–910

Knickmeyer RC, Gouttard S, Kang C, Evans D, Wilber K, Smith JK, Hamer RM, Lin W, Gerig G, Gilmore JH (2008) A structural MRI study of human brain development from birth to 2 years. J Neurosci 28(47):12176–12182

Kong X-Z, Postema MC, Guadalupe T, de Kovel C, Boedhoe PS, Hoogman M, Mathias SR, Van Rooij D, Schijven D, Glahn DC

et al (2020) Mapping brain asymmetry in health and disease through the enigma consortium. Hum Brain Map 2020:1–15
Kreitzer AC, Malenka RC (2008) Striatal plasticity and basal ganglia circuit function. Neuron 60(4), 543–554
Langsrud Ø (2003) Anova for unbalanced data: Use type ii instead of type iii sums of squares. Statistics and Computing 13(2), 163–167
Lashley KS (1958) Cerebral organization and behavior. Res Publ Assoc Res Nerv Mental Dis 36:1–18
LeDoux JE, Michel M, Lau H (2020) A little history goes a long way toward understanding why we study consciousness the way we do today. Proc Natl Acad Sci 117(13):6976–6984
Leonard CM, Eckert MA (2008) Asymmetry and dyslexia. Developmental neuropsychology 33(6):663–681
Liu FT, Ting KM, Zhou Z-H (2008) Isolation forest. In: 2008 eighth IEEE international conference on data mining, pp 413–422. IEEE
Lotze M, Domin M, Gerlach FH, Gaser C, Lueders E, Schmidt CO, Neumann N (2019) Novel findings from 2,838 adult brains on sex differences in gray matter brain volume. Scientific reports 9(1):1–7
McLachlan RS (2009) A brief review of the anatomy and physiology of the limbic system. Can J Neurol Sci 36:S84
Mendrek A (2007) Reversal of normal cerebral sexual dimorphism in schizophrenia: evidence and speculations. Med Hypotheses 69(4):896–902
Morillon B, Lehongre K, Frackowiak RS, Ducorps A, Kleinschmidt A, Poeppel D, Giraud A-L (2010) Neurophysiological origin of human brain asymmetry for speech and language. Proc Natl Acad Sci 107(43):18688–18693
Narvacan K, Treit S, Camicioli R, Martin W, Beaulieu C (2017) Evolution of deep gray matter volume across the human lifespan. Hum Brain Map 38(8):3771–3790
Neubauer S, Gunz P, Scott NA, Hublin J-J, Mitteroecker P (2020) Evolution of brain lateralization: a shared hominid pattern of endocranial asymmetry is much more variable in humans than in great apes. Sci Adv 6(7):eaax9935
Nickl-Jockschat T, Kleiman A, Schulz JB, Schneider F, Laird AR, Fox PT, Eickhoff SB, Reetz K (2012) Neuroanatomic changes and their association with cognitive decline in mild cognitive impairment: a meta-analysis. Brain Struct Funct 217(1):115–125
Nielsen JA, Zielinski BA, Ferguson MA, Lainhart JE, Anderson JS (2013) An evaluation of the left-brain vs. right-brain hypothesis with resting state functional connectivity magnetic resonance imaging. PloS One 8(8):e71275
Nobis L, Manohar SG, Smith SM, Alfaro-Almagro F, Jenkinson M, Mackay CE, Husain M (2019) Hippocampal volume across age: nomograms derived from over 19,700 people in uk biobank. NeuroImage Clin 23:101904
Núñez C, Theofanopoulou C, Senior C, Cambra MR, Usall J, Stephan-Otto C, Brébion G (2018) A large-scale study on the effects of sex on gray matter asymmetry. Brain Struct Funct 223(1), 183–193
Ocklenburg S, Gunturkun O (2012) Hemispheric asymmetries: the comparative view. Front Psychol 3:5
Okada N, Yahata N, Koshiyama D, Morita K, Sawada K, Kanata S, Fujikawa S, Sugimoto N, Toriyama R, Masaoka M et al. (2018) Abnormal asymmetries in subcortical brain volume in early adolescents with subclinical psychotic experiences. Transl Psychiatry 8(1):1–11
Palmer AR (2004) Symmetry breaking and the evolution of development. Science 306(5697):828–833
Pedregosa F, Varoquaux G, Gramfort A, Michel V, Thirion B, Grisel O, Blondel M, Prettenhofer P, Weiss R, Dubourg V, Vanderplas J, Passos A, Cournapeau D, Brucher M, Perrot M, Duchesnay E (2011) Scikit-learn: machine learning in Python. J Mach Learn Res 12:2825–2830
Rane S, Plassard A, Landman BA, Claassen DO, Donahue MJ (2017) Comparison of cortical and subcortical measurements in normal older adults across databases and software packages. J Alzheimer's Dis Rep 1(1):59–70
Ritchie SJ, Cox SR, Shen X, Lombardo MV, Reus LM, Alloza C, Harris MA, Alderson HL, Hunter S, Neilson E et al. (2018) Sex differences in the adult human brain: evidence from 5216 uk biobank participants. Cereb Cortex 28(8):2959–2975
Roalf DR, Vandekar SN, Almasy L, Ruparel K, Satterthwaite TD, Elliott MA, Podell J, Gallagher S, Jackson CT, Prasad K et al. (2015) Heritability of subcortical and limbic brain volume and shape in multiplex-multigenerational families with schizophrenia. Biol Psychiatry 77(2):137–146
Ruigrok AN, Salimi-Khorshidi G, Lai M-C, Baron-Cohen S, Lombardo MV, Tait RJ, Suckling J (2014) A meta-analysis of sex differences in human brain structure. Neurosci Biobehav Rev 39:34–50
Seabold S, Perktold J (2010) statsmodels: econometric and statistical modeling with python. In: 9th python in science conference
Shaw C-M, Alvord EC Jr (1997) Neuropathology of the limbic system. Neuroimaging Clin North Am 7(1), 101–142
Sperry RW (1961) Cerebral organization and behavior. Science 133(3466):1749–1757
Sperry RW (1984) Consciousness, personal identity and the divided brain. Neuropsychologia 133(3466):1749–1757
Szabó CÁ, Lancaster JL, Xiong J, Cook C, Fox P (2003) Mr imaging volumetry of subcortical structures and cerebellar hemispheres in normal persons. Am J Neuroradiol 24(4), 644–647
Tang X, Holland D, Dale AM, Miller MI (2015) Apoe affects the volume and shape of the amygdala and the hippocampus in mild cognitive impairment and Alzheimer's disease: age matters. J Alzheimer's Dis 47(3):645–660
van der Knaap LJ, van der Ham IJ (2011) How does the corpus callosum mediate interhemispheric transfer? a review. Behav Brain Res 223(1):211–221
Vos M, Starmans M, Timbergen M, van der Voort S, Padmos G, Kessels W, Niessen W, van Leenders G, Grünhagen D, Sleijfer S et al (1800) (2019) Radiomics approach to distinguish between well differentiated liposarcomas and lipomas on mri. Br J Surg 106(13):1800–1809
Wen W, Thalamuthu A, Mather KA, Zhu W, Jiang J, De Micheaux PL, Wright MJ, Ames D, Sachdev PS (2016) Distinct genetic influences on cortical and subcortical brain structures. Sci Rep 6(1):1–11
Willems RM, Peelen MV, Hagoort P (2010) Cerebral lateralization of face-selective and body-selective visual areas depends on handedness. Cereb Cortex 20(7):1719–1725